



Research Paper

ROS via BTK-p300-STAT1-PPAR γ signaling activation mediates cholesterol crystals-induced CD36 expression and foam cell formation



Sivareddy Kotla, Nikhlesh K. Singh, Gadiparthi N. Rao*

Department of Physiology, University of Tennessee Health Science Center, Memphis, TN 38163, USA

A B S T R A C T

In understanding the mechanisms of cholesterol in the pathogenesis of atherosclerosis, previous studies from other laboratories have demonstrated that cholesterol crystals (CC) induce scavenger receptor CD36 expression and NLRP3-mediated inflammasome formation. In elucidating the mechanisms by which CC could enhance CD36 expression and foam cell formation, here we report that CC via NADPH and xanthine oxidases-mediated ROS production activates BTK, a non-receptor tyrosine kinase. In addition, CC induce p300 tyrosine phosphorylation and activation in a BTK-dependent manner, which in turn, leads to STAT1 acetylation and its interaction with PPAR γ in CD36 expression, oxLDL uptake and foam cell formation. Furthermore, p300, STAT1 and PPAR γ bound to a STAT binding site at –107 nt in CD36 promoter and enhanced its activity in ROS and BTK-dependent manner. Disruption of this STAT binding site by site-directed mutagenesis abolished CC-induced CD36 promoter activity. Together these results reveal for the first time that CC via producing ROS and activating BTK causes p300-mediated STAT1 acetylation and its interaction with PPAR γ in CD36 expression, oxLDL uptake and foam cell formation.

1. Introduction

Atherosclerosis is a chronic inflammatory disease of the arterial wall and is one of the leading causes of death worldwide [1,2]. Atherosclerosis is characterized by accumulation of lipid-laden foam cells in the subendothelial space and calcification of the plaque [2,3]. Scavenger receptors play an important role in foam cell formation because of their ability to bind to and internalize oxidized (ox)-LDL [1–4]. In humans, two major classes of scavenger receptors have been identified and designated as type A and type B receptors [5]. CD36, a cell surface glycoprotein is a member of the scavenger receptor type B family, which also includes SR-B1 and HDL receptor [6]. CD36 is expressed in various cell types including monocytes [7,8], endothelial cells [9], platelets [10] and adipocytes [11]. CD36 recognizes a variety of ligands including oxLDL [7], anionic-phospholipids [6] and collagen [10].

Cholesterol in the form of cholesterol crystals (CC) plays an important role in the atherosclerotic lesion formation, for which reason, it is classified as a prognostic marker for atherosclerosis [12]. Several studies have reported that CC are present at the sites of plaque rupture, suggesting an important link between plasma cholesterol levels and the pathogenesis of atherosclerosis [13–15]. Many studies have also reported the involvement of CC in the early atherosclerotic lesion formation [12]. The role of CC in the pathogenesis of atherosclerosis

can also be eluded by the finding that CC induce NALP3-mediated inflammasome formation [12]. In addition, the role of CC in complement-dependent reactive oxygen species and proinflammatory cytokine production has been reported [16] and there is a large body of evidence that connects oxidant stress to the pathogenesis of a variety of diseases including cardiovascular diseases [17]. Furthermore, several studies have demonstrated that cholesterol enhances CD36 expression supporting its role in foam cell formation [18,19]. However, the mechanisms by which cellular cholesterol induces CD36 expression were not explored. In this context, we have studied the mechanisms by which CC could induce CD36 expression, oxLDL uptake and foam cell formation. In this study, we report that CC induce CD36 expression, oxLDL uptake and foam cell formation via STAT1 acetylation and its interaction with PPAR γ . We also show that STAT1 acetylation requires ROS-dependent BTK-mediated p300 tyrosine phosphorylation and activation.

2. Materials and methods

2.1. Reagents

LDH cytotoxicity assay kit (601170) and MTT cell proliferation assay kit (10009365) were purchased from Cayman chemical (Ann Arbor, MI). Anti-phosphoserine/threonine (ab17464) and anti-Pyk2

* Correspondence to: Department of Physiology, University of Tennessee Health Science Center, 894 Union Avenue, Memphis, TN 38163, USA.
E-mail address: rgadipar@uthsc.edu (G.N. Rao).

<http://dx.doi.org/10.1016/j.redox.2016.12.005>

Received 18 October 2016; Received in revised form 28 November 2016; Accepted 2 December 2016

Available online 07 December 2016

2213-2317/ © 2016 The Authors. Published by Elsevier B.V.

This is an open access article under the CC BY-NC-ND license (<http://creativecommons.org/licenses/by-nc-nd/4.0/>).

(ab32571) antibodies were obtained from Abcam (Cambridge, MA). Anti-pBTK (5082), anti-pPyk2 (3291), anti-pSrc (2101), anti-pSTAT1 (9177), anti-pSTAT2 (4441), anti-pSTAT3 (9133), anti-pSTAT4 (5267), anti-pSTAT5 (9351), anti-pSTAT6 (9364), and anti-pSyk (2715) antibodies were bought from Cell Signaling Technology (Beverly, MA). Anti-acetyl lysine (SC-32268), anti-BTK (SC-1696), anti-CD36 (SC-9154), anti-CBP (SC-369), anti-p300 (SC-584), anti-PPAR α (SC-9000), anti-PPAR β (SC-7197), anti-PPAR γ (SC-7196), anti-p47Phox (SC14015), anti-SR-A1 (SC-9104), anti-SR-B1 (SC-67098), anti-STAT1 (SC-464), anti-STAT2 (SC-476), anti-STAT3 (SC-482), anti-STAT4 (SC-486), anti-STAT5 (SC-835), anti-STAT6 (SC-981), anti-Syk (SC-573), anti- β -tubulin (SC-9104) and anti-xanthine oxidase (SC-20991) antibodies as well as normal mouse serum (SC-45051) and normal rabbit serum (SC-3888) were purchased from Santa Cruz Biotechnology (Santa Cruz, CA). Anti-PPAR δ antibodies (NBP1-39684) were obtained from Novus Biologicals (Littleton, CO). Anti-phosphotyrosine antibodies (05-777) and p300 immunoprecipitation-HAT assay kit (17-284) were procured from Millipore Corporation (Temecula, CA). Diphenyleneiodonium chloride (BML-CN240) was bought from Enzo Life Science (Farmingdale, NY). Acetyl coenzyme A (A2056), Apocyanin (A10809), Allopurinol (A8003), Cholesterol (C8667) and Oil red O (234117) were purchased from Sigma-Aldrich Chemicals (St. Louis, MO). Amplex Red hydrogen peroxide/peroxidase assay kit (A22188), CM-H2DCFDA [5-(and 6)-chloromethyl-2', 7'-dichlorodihydrofluorescein diacetate acetyl ester] (C6827), GW9662 (1508) and Lipofectin transfection reagent (15596018) were obtained from Invitrogen (Grand Island, NY). pGL3 basic vector and luciferase assay system (E4530) were bought from Promega (Madison, WI). Dil-oxLDL (BT-920) and oxLDL (BT-910) were obtained from Biomedical Technologies (Stoughton, MA). Biotin 3' End DNA labeling Kit (89818) and Lightshift Chemiluminescent EMSA Kit (20148) were procured from Pierce Biotechnology (Rockford, IL). The enhanced chemiluminescence (ECL) Western blotting detection reagents (RPN2106) were obtained from GE Healthcare. [3 H]-Acetyl CoA (S.A. 8.6 Ci/mmol) was purchased from Perkin Elmer (Waltham, MA). All the phosphorothioate-modified antisense oligonucleotides (ASOs) and primers were synthesized by IDT (Coralville, IA). The phosphorothioate-modified ASOs used in this study are as follows: hControl ASO, 5'-GGGGUTCTCTGCGTACGGTGCUAGU-3'; hCBP (NM_001020603) ASO, 5'-GCGUUAGGGTCACAGCAGC-3'; hCD36 (NM_000072) ASO, 5'-CCACAGTTCGGTCACAGCC-3'; hp47Phox (NM_000265) ASO, 5'-GUUGGGCTCAGGTCTTCCGUCUC-3'; hPyk2 (NM_173175) ASO, 5'-CCUGUGTCCATAGCCAGAGUACC-3'; hp300 (NM_004380) ASO, 5'-UGUGUUGTTGGTGTAGGUGU-3'; and hXO (NM_000379) ASO, 5'-GCCUCCTCCATTCTCTCACUCG-3'.

2.2. Cell culture

THP1 cells, a human leukemic monocyte cell line, were purchased from American Type Culture Collection (Manassas, VA) and cultured in RPMI-1640 medium supplemented with 10% heat-inactivated fetal bovine serum (FBS), 50 U/ml penicillin, 50 μ g/ml streptomycin and 50 μ M β -mercaptoethanol. To perform the experiments, cells were growth-arrested in serum-free RPMI-1640 medium containing the antibiotics and β -mercaptoethanol overnight. Cultures were maintained in a humidified 95% air and 5% CO $_2$ atmosphere at 37 $^{\circ}$ C.

2.3. Preparation of cholesterol crystals

Cholesterol crystals were prepared according to the method of Flynn et al. [20]. Briefly, cholesterol was dissolved in 95% ethanol (12.5 g/l), heated at 60 $^{\circ}$ C for 2 h, filtered through Whatman filter paper and left at room temperature for crystallization. Crystals were collected by filtering, grinded with autoclaved mortar and pestle to yield 1–10 μ m in size, and stored at -20 $^{\circ}$ C.

2.4. Mouse primary peritoneal macrophage isolation

Mouse primary peritoneal macrophages were isolated as described by us previously [21].

2.5. Cell cytotoxicity

Cell cytotoxicity was measured by LDH release using a kit and following the manufacturer's protocol.

2.6. Cell proliferation assay

Cell proliferation was measured by MTT assay following the manufacturer's protocol.

2.7. RT-PCR

Total cellular RNA was extracted from THP1 cells using TRIzol reagent according to the manufacturer's protocol. Reverse transcription was performed with a high capacity cDNA reverse transcription kit (Applied Biosystems). Complementary DNA (cDNA) was then used as a template for amplification using the following primers: human SR-A1 (NM_002445), forward, 5'-CCTCGTGTTCGAGTTCCTCA-3' and reverse, 5'-CCATGTTGCTCATGTGTTCC-3'; human SR-B1 (NM_001082959), forward, 5'-CTGTGGGTGAGATCATGTGG-3' and reverse, 5'-GCCCTTCCTTTGGAGTAACC-3'; human CD36 (NM_000072), forward, 5'-ACAGATGCAGCCTCATTTC-3' and reverse, 5'-GCCTTGGATGGAAGAACAAA-3'; human β -actin (NM_001101), forward, 5'-AGCCATGTACGTTGCTAT-3' and reverse, 5'-GATGTCCACGTCACACTCA-3'. The amplification was performed using Gene AMP PCR system 2400 (Applied Biosystems). The amplified PCR products were separated on 1.5% agarose gels, stained with ethidium bromide and the images were captured using a Kodak In Vivo Imaging System.

2.8. Western blotting

Cell extracts containing an equal amount of protein from control and the indicated treatments were resolved by electrophoresis on 0.1% (W/V) SDS and 10% (W/V) polyacrylamide gels. The proteins were transferred electrophoretically to a nitrocellulose membrane. After blocking in either 5% (W/V) nonfat dry milk or 5% (W/V) BSA, the membrane was probed with appropriate primary antibodies followed by incubation with Horseradish Peroxidase-conjugated secondary antibodies. The antigen-antibody complexes were detected using enhanced chemiluminescence detection reagent kit (GE Health Care).

2.9. Acetyl transferase assay

The acetyl transferase activity of p300 was measured using a kit as per the supplier's protocol.

2.10. ROS

Intracellular ROS production was measured using membrane permeable CM-H2DCFDA as well as Amplex Red Hydrogen Peroxide/Peroxidase Assay Kit as described previously [21,22].

2.11. Transfections

Transfections were performed as described previously [23]. Briefly, cells were transfected with the indicated ASOs at 100 nM concentration using Lipofectin transfection reagent for 6 h following the manufacturer's instructions. After transfection, cells were maintained in complete RPMI-1640 medium for 36 h followed by growth arresting in serum-free medium overnight before using for experiments.

2.12. Cloning and mutagenesis

Human CD36 promoter cloning and its site-directed mutagenesis of STAT1 K410R/K413R were described previously [23].

2.13. EMSA

Nuclear extracts of THP1 cells with and without appropriate treatments were prepared as described previously [23]. The protein content of the nuclear extracts was determined using a micro-BCA method (Pierce Biotechnology). Biotin-labeled double-stranded oligonucleotides encompassing STAT-binding element at -107 nt forward (5'-ATTTTTTTTCTTTC AATTTCTCTAGGA AACAAACCACACTG-3'), reverse (5'-CAGTGTGTGGTTTGTTC CTAGA GAAATTGAAAGAAAAAAAAT-3') were used as a probe. Briefly, 5 µg of nuclear extract was incubated in a binding buffer (10 mM Tris-HCl, pH 7.9, 50 mM KCl, 1 mM DTT, 15% glycerol) with 2.5 nM of biotin-labeled probe and 2 µg of poly dI: dC for 30 min at room temperature in a total volume of 20 µl on ice and the DNA-protein complexes were analyzed by electrophoresis on 6% polyacrylamide gels and visualized by chemiluminescence imaging. To perform a supershift EMSA, the complete reaction mix was incubated with 2 µg of the indicated antibody for 1 h on ice before separating it by electrophoresis. Normal serum was used as a negative control.

2.14. Luciferase assay

THP1 cells were co-transfected with pGL3 empty vector, pGL3-hCD36 or pGL3-hCD36m promoter along with the indicated plasmids using Lipofectamine transfection reagent. After growth arresting in serum-free medium for 12 h, cells were treated with and without 40 µg CC for 6 h, washed with cold PBS and lysed in 200 µl of lysis buffer. The cell extracts were cleared by centrifugation at 12,000 rpm for 2 min at 4 °C. The supernatants were assayed for luciferase activity using luciferase assay system (Promega) and a single tube luminometer (TD20/20; Turner Designs, Sunnyvale, CA) and expressed as relative luciferase units (RLU).

2.15. Chromatin immunoprecipitation (ChIP) and Re-ChIP assays

ChIP assay was performed on THP1 cells with and without the indicated treatments using a kit and following the supplier's protocol (Upstate Biotechnology Inc., Lake Placid, NY). STAT1, PPAR γ and p300-DNA complexes were immunoprecipitated using anti-STAT1, anti-PPAR γ and anti-p300 antibodies, respectively. Pre-immune mouse serum or rabbit serum were used as negative controls. For chromatin re-immunoprecipitation (*re*-ChIP) assay, the chromatin complexes were eluted from the first ChIP with 10 mM DTT at 37 °C for 30 min and diluted 20 times with ChIP dilution buffer (1% Triton X-100, 2 mM EDTA, 20 mM Tris-HCl, pH 8.1 and 150 mM NaCl) and immunoprecipitated with the indicated antibodies. In the case of *Re*-ChIP, chromatin was immunoprecipitated in a sequential manner with the indicated antibodies. The immunoprecipitated DNA was uncross-linked, subjected to Proteinase K digestion, purified using QIAquick columns (Cat. No. 28104, Qiagen, Valenica, CA). The ChIP and *re*-ChIP samples were analyzed by PCR by using the following primers: forward, 5'-GGGGAACTCAGCAAGTCAG-3' and reverse, 5'-AGTGTGATCCCAGTGG-3' that would amplify 228 bp fragment encompassing the STAT-binding site at -107 nt. The resulting PCR products were resolved on 1.8% agarose gels, stained with ethidium bromide and the images were captured using Kodak In Vivo Imaging System.

2.16. Dil-oxLDL uptake assay

Dil-oxLDL uptake was measured according to the method of McLaren et al. [24]. Briefly, THP1 cells with and without the indicated treatments were incubated with Dil-oxLDL (10 µg/ml) for 6 h at 37 °C.

After incubation with Dil-oxLDL, cells were washed with PBS, resuspended in PBS and analyzed by FACSCalibur flow cytometer (BD Biosciences, San Jose, CA) with an acquired capacity of 10,000 cells. The data were analyzed using cellquest software and Dil-oxLDL uptake is presented as a percentage of the total cells.

2.17. Foam cell assay

Foam cell formation was performed as per the method of McLaren et al. [24]. Briefly, THP1 cells that were treated with and without the indicated treatments were incubated with oxLDL (10 µg/ml) for 6 h at 37 °C. Cells were then fixed with 4% paraformaldehyde for 30 min, stained with Oil red O for 10 min and counterstained with hematoxylin. Cell staining was observed under a Nikon Eclipse 50i microscope with 40X/0.65 magnification and the images were captured with a Nikon Digital Slight DS-L1 camera. After capturing the images, the Oil red O stain was eluted by incubating the slides with isopropanol for 15 min at room temperature and the optical density was measured at 500 nm in a SpectraMax 190 spectrophotometer (Molecular Devices).

2.18. Statistics

All the experiments were repeated three times and the data are presented as Mean \pm S.D. The treatment effects were analyzed by Student *t*-test, and the *p* values < 0.05 were considered statistically significant. In the case of EMSA, supershift EMSA and Western blotting, one representative set of data is shown.

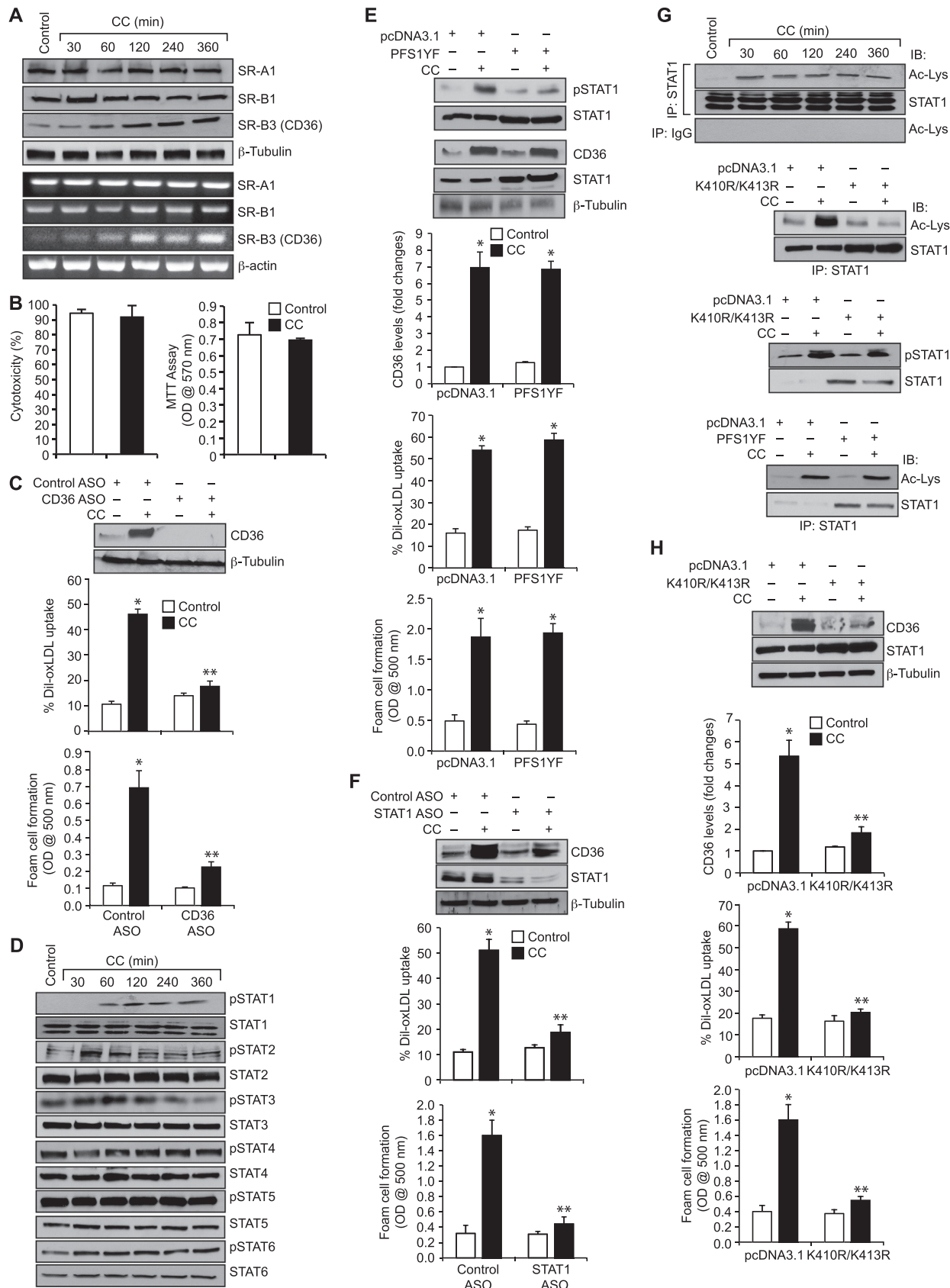
3. Results

3.1. Role of STAT1 acetylation in CC-induced CD36 expression, oxLDL uptake and foam cell formation

CD36 plays a crucial role in foam cell formation, one of the underlying factors in atherogenesis [25,26]. The presence of CC in the advanced atherosclerotic lesions of human and animal models and its effects on CD36 expression suggest a role for cholesterol in atherogenesis [13–15]. To understand the mechanisms by which CC regulate foam cell formation, we have studied its effects on scavenger receptor expression in human monocytic THP1 cells. CC while having no effect on SR-A1 and SR-B1 expression, induced the expression of CD36 at both protein and mRNA levels in a time dependent manner with maximum effects at 4 h and 2 h, respectively (Fig. 1A). CC neither exhibited cytotoxic effects in THP1 cells nor influenced their proliferation (Fig. 1B). Since, CC-induced CD36 expression, we have studied its role in oxLDL uptake and foam cell formation. Anti-sense oligonucleotide (ASO)-mediated downregulation of CD36 levels attenuated CC-induced oxLDL uptake and foam cell formation (Fig. 1C). These results suggest that CC induce oxLDL uptake and foam cell formation via CD36 expression. Studies from others as well as our laboratories have shown a role for STAT1 in CD36 expression [27,28]. To test the role of STATs in CC-induced CD36 expression, oxLDL uptake and foam cell formation, we have studied the effects of CC on STAT1, STAT2, STAT3, STAT4, STAT5 and STAT6 activation. CC while having no major effect on STAT2, STAT3, STAT4, STAT5 and STAT6 tyrosine phosphorylation induced STAT1 tyrosine phosphorylation (Fig. 1D). This finding suggests that CC activate STAT1. However, blockade of STAT1 tyrosine phosphorylation using its dominant negative tyrosine mutant PFS1YF [29] had no effect on CC-induced CD36 expression, oxLDL uptake and foam cell formation (Fig. 1E). These findings indicate that tyrosine phosphorylation of STAT1 had no influence on CC-induced CD36 expression, oxLDL uptake and foam cell formation. However, ASO-mediated depletion of STAT1 levels attenuated CC-induced CD36 expression, oxLDL uptake and foam cell formation (Fig. 1F). Many studies have shown that besides phosphorylation, acetylation plays a role in the activation of STATs, particularly STAT1 and

STAT3 [30–32]. Based on this information, we have tested the effect of CC on STAT1 acetylation. CC induced STAT1 acetylation in a time dependent manner (Fig. 1F). STAT1 gets acetylated at K410/K413

residues [29]. To identify the potential lysine residue(s) of STAT1 that are acetylated by CC, we tested the effect of K410R/K413R mutant on CC-induced STAT1 acetylation. Transfection of cells with K410R/



K413R mutant blocked CC-induced STAT1 acetylation (Fig. 1G), suggesting that STAT1 is acetylated at K410/K413 residues in response to CC. To find whether STAT1 acetylation has any role in STAT1 tyrosine phosphorylation, we tested the effect of K410R/K413R mutant on CC-induced STAT1 tyrosine phosphorylation. STAT1 K410R/K413R mutant had no effect on CC-induced STAT1 tyrosine phosphorylation (Fig. 1G). To find whether there is any link between STAT1 tyrosine phosphorylation and its acetylation, we next tested the effect of its tyrosine dominant negative mutant PFS1YF. PFS1YF had no effect on CC-induced STAT1 acetylation (Fig. 1G). These findings indicate that STAT1 tyrosine phosphorylation and acetylation are triggered independent of each other by CC. To find whether STAT1 acetylation has any role in CC-induced CD36 expression, oxLDL uptake and foam cell formation, we tested the effect of K410R/K413R mutant. Transfection of cells with K410R/K413R mutant blocked CC-induced CD36 expression, oxLDL uptake and foam cell formation (Fig. 1H).

3.2. Role of STAT1 acetylation in the recruitment of PPAR γ in CC-induced CD36 expression, oxLDL uptake and foam cell formation

A large body of evidence suggests that PPAR γ mediates CD36 expression in response to its ligands, including 15(S)-HETE [33–35]. To find the role of PPAR γ in CC-induced CD36 expression, we tested the effect of PPAR γ antagonist GW9662 [33]. GW9662 inhibited CC-induced CD36 expression, oxLDL uptake and foam cell formation (Fig. 2A). Since both STAT1 acetylation and PPAR γ activation are involved in CC-induced CD36 expression, oxLDL uptake and foam cell formation, we wanted to explore whether PPAR γ activation is required for CC-induced STAT1 acetylation. However, blockade of PPAR γ activation by GW9662 had no effect on CC-induced STAT1 acetylation (Fig. 2B). To understand how CC induced CD36 expression by recruiting two different transcriptional factors, we asked the question whether there is any interaction between these transcriptional factors. Co-immunoprecipitation experiment revealed that STAT1 exists in complex with PPAR α , PPAR β and PPAR δ constitutively and in response to CC its association with PPAR γ increases in a time dependent manner with maximum effect at 1 h (Fig. 2B). Conversely, PPAR γ formed a complex with STAT2, STAT4, and STAT6 constitutively and in response to CC its association with STAT1 increases in a time dependent manner (Fig. 2B). In order to test the role of STAT1 tyrosine phosphorylation and acetylation on its interaction with PPAR γ , we tested the effect of its tyrosine and acetyl mutants, PFS1YF and K410R/K413R, respectively. PFS1YF mutant had no effect on CC-induced STAT1 association with PPAR γ (Fig. 2C). On the other hand, K410R/K413R mutant blocked CC-induced STAT1 association with PPAR γ (Fig. 2C). These findings indicate that STAT1

acetylation but not tyrosine phosphorylation is required for its interaction with PPAR γ .

3.3. Role of p300 in CC-induced STAT1 acetylation and its interaction with PPAR γ in CD36 expression, oxLDL uptake and foam cell formation

Previously, we have demonstrated a role for p300 in 15(S)-HETE-induced STAT1 acetylation and its interaction with PPAR γ in CD36 expression, oxLDL uptake and foam cell formation [23]. Therefore, to understand the mechanisms by which CC regulate STAT1 acetylation, we have studied the role of p300. Co-immunoprecipitation experiments showed that while p300 exists in complex with both STAT3 and STAT5 basally its association with STAT1 increases in a time dependent manner in response to CC (Fig. 3A). No significant changes were noted between STAT3 or STAT5 interaction with p300 in response to treatment with CC (Fig. 3A). Furthermore, downregulation of p300 using its ASO inhibited CC-induced STAT1 acetylation and its interaction with PPAR γ (Fig. 3B). In addition, p300 downregulation inhibited CC-induced CD36 expression, oxLDL uptake and foam cell formation (Fig. 3C). To confirm the role of p300 acetyltransferase activity in STAT1 acetylation and its interaction with PPAR γ in CD36 expression, oxLDL uptake and foam cell formation, we tested the effect of p300 Δ HAT mutant that lacks acetyltransferase activity [36]. While transfection of cells with p300 WT increased CC-induced STAT1 acetylation and its interaction with p300 leading to enhanced CD36 expression, oxLDL uptake and foam cell formation, transfection of cells with p300 Δ HAT mutant prevented these effects (Fig. 3D and E). To test the specificity of p300 in CC-induced STAT1 acetylation and its interaction with PPAR γ in CD36 expression and oxLDL uptake, we next studied the role of its homologue CBP. ASO-mediated downregulation of CBP levels had no effect on CC-induced STAT1 acetylation, its interaction with PPAR γ , CD36 expression and oxLDL uptake (Fig. 3F and G).

3.4. Role of BTK in CC-induced p300 tyrosine phosphorylation, STAT1 acetylation and its interaction with PPAR γ in CD36 expression, oxLDL uptake and foam cell formation

To decipher the mechanism(s) by which CC modulate p300 activation, we studied its effects on p300 phosphorylation. CC while having no effect on p300 serine/threonine phosphorylation induced its tyrosine phosphorylation in a time dependent manner (Fig. 4A). Previously, we have shown that non-receptor tyrosine kinases (NRTKs) Syk and Pyk2 were involved in 15(S)-HETE-induced p300 tyrosine phosphorylation and its activation leading to STAT1 acetylation and its interaction with PPAR γ in CD36 expression, oxLDL uptake and foam cell formation [27]. To identify NRTK that mediates

Fig. 1. CC-induced CD36 expression, oxLDL uptake and foam cell formation require STAT1 acetylation. A. Quiescent cells were treated with vehicle or CC (40 μ g/ml) for the indicated time periods and either protein extracts were prepared or RNA was isolated. The protein extracts and RNA were analyzed by Western blotting and RT-PCR for the indicated scavenger receptors expression and normalized to β -tubulin protein and β -actin mRNA levels, respectively. B. Cells were treated with vehicle or CC (40 μ g/ml) for 6 h and tested for their cytotoxicity and proliferation by LDH release and MTT assays, respectively. C. Upper panel: Cells were transfected with the indicated ASO, quiesced, treated with vehicle or CC for 4 h and analyzed by Western blotting for CD36 levels and the blot was reprobed for β -tubulin to show the effects of the ASO on its target and off target molecules levels. Middle and bottom panels: All the conditions were the same as in the upper panel except that cells were subjected to CC-induced oxLDL uptake (middle panel) or foam cell formation (bottom panel) assays. D. Equal amounts of protein from control and various time periods of CC-treated cells were analyzed by Western blotting for pSTAT1, pSTAT2, pSTAT3, pSTAT4, pSTAT5 and pSTAT6 levels and normalized to their total levels. E. Upper panel: Cells were transfected with vector or PFS1YF, quiesced, treated with and without CC for 1 h or 4 h, cell extracts were prepared and analyzed by Western blotting for pSTAT1 (1 h samples) and CD36 levels (4 h samples) and the blots were reprobed for STAT1 over expression and β -tubulin normalization. Middle and bottom panels: All the conditions were the same as in the upper panel except that after quiescence cells were subjected to CC-induced oxLDL uptake (middle panel) and foam cell formation (bottom panel) assays. F. Cells were transfected with control or STAT1 ASO, quiesced, treated with and without CC and analyzed for CD36 expression, oxLDL uptake or foam cell formation as described in panel C. The CD36 blot was reprobed for STAT1 and β -tubulin to show the effect of the ASO on its target and off target molecules levels. G. Upper panel: Equal amounts of proteins from control and the indicated time periods of CC-treated cells were immunoprecipitated with anti-STAT1 antibodies or IgG and the immunocomplexes were analyzed by Western blotting using anti-acetyl lysine (Ac-Lys) antibodies followed by normalization to STAT1. Lower panels: Cells were transfected with vector, K410R/K413R or PFS1YF, quiesced, treated with and without CC for 1 h and analyzed for STAT1 acetylation and phosphorylation as described in the upper panel and panel C, respectively and the blots were reprobed for STAT1 levels. H. Cells were transfected with vector or K410R/K413R, quiesced, treated with and without CC and analyzed for CD36 expression, oxLDL uptake or foam cell formation as described in panel C. The bar graphs represent Mean \pm S.D. values of three experiments. * $p < 0.01$ vs vehicle control or vector control or control ASO; ** $p < 0.01$ vs CC or control ASO+CC or vector control+CC.

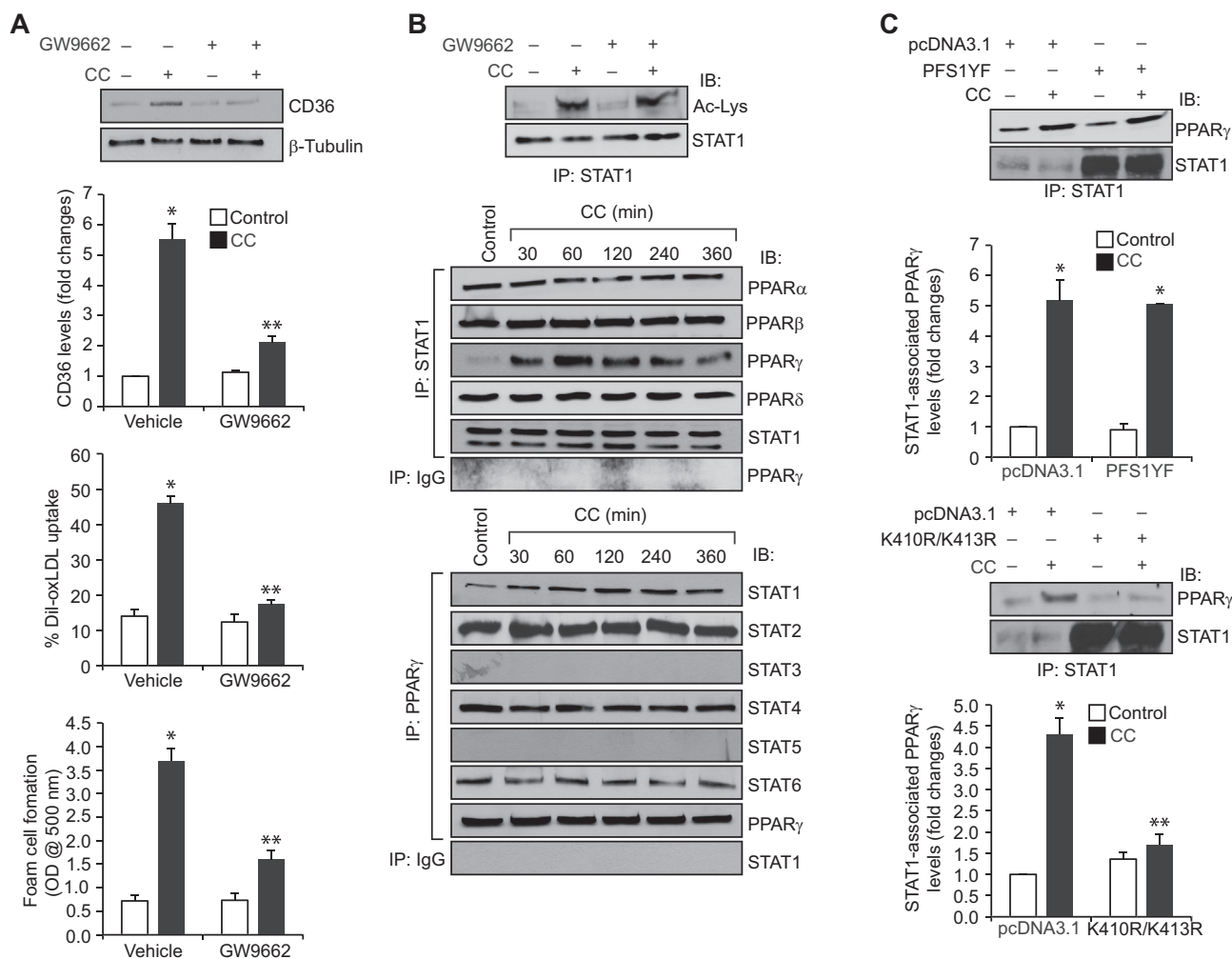


Fig. 2. CC-induced CD36 expression, oxLDL uptake and foam cell formation require STAT1 interaction with PPAR γ . **A.** Quiescent cells were treated with vehicle or CC (40 μ g/ml) in the presence and absence of GW9662 (5 μ M) and analyzed for CD36 expression, oxLDL uptake or foam cell formation as described in Fig. 1, panel C. **B.** Upper panel: Quiescent cells were treated with and without CC in the presence and absence of GW9662 for 1 h and analyzed for STAT1 acetylation as described in Fig. 1, panel F. Middle and bottom panels: Equal amounts of protein from control and the indicated time periods of CC-treated cells were immunoprecipitated with anti-STAT1 or anti-PPAR γ antibodies or IgG and the immunocomplexes were analyzed by Western blotting for the indicated proteins using their specific antibodies and normalized for STAT1 or PPAR γ . **C.** Cells were transfected with vector, PFS1YF or K410R/K413R, quiesced, treated with and without CC for 1 h and equal amounts of protein from control and each treatment were immunoprecipitated with anti-STAT1 antibodies and the immunocomplexes were analyzed by Western blotting for PPAR γ . The blots were reprobed for STAT1 over expression. The bar graphs represent Mean \pm S.D. of three experiments * p < 0.01 vs vehicle control or vector control; ** p < 0.01 vs CC or vector control+CC.

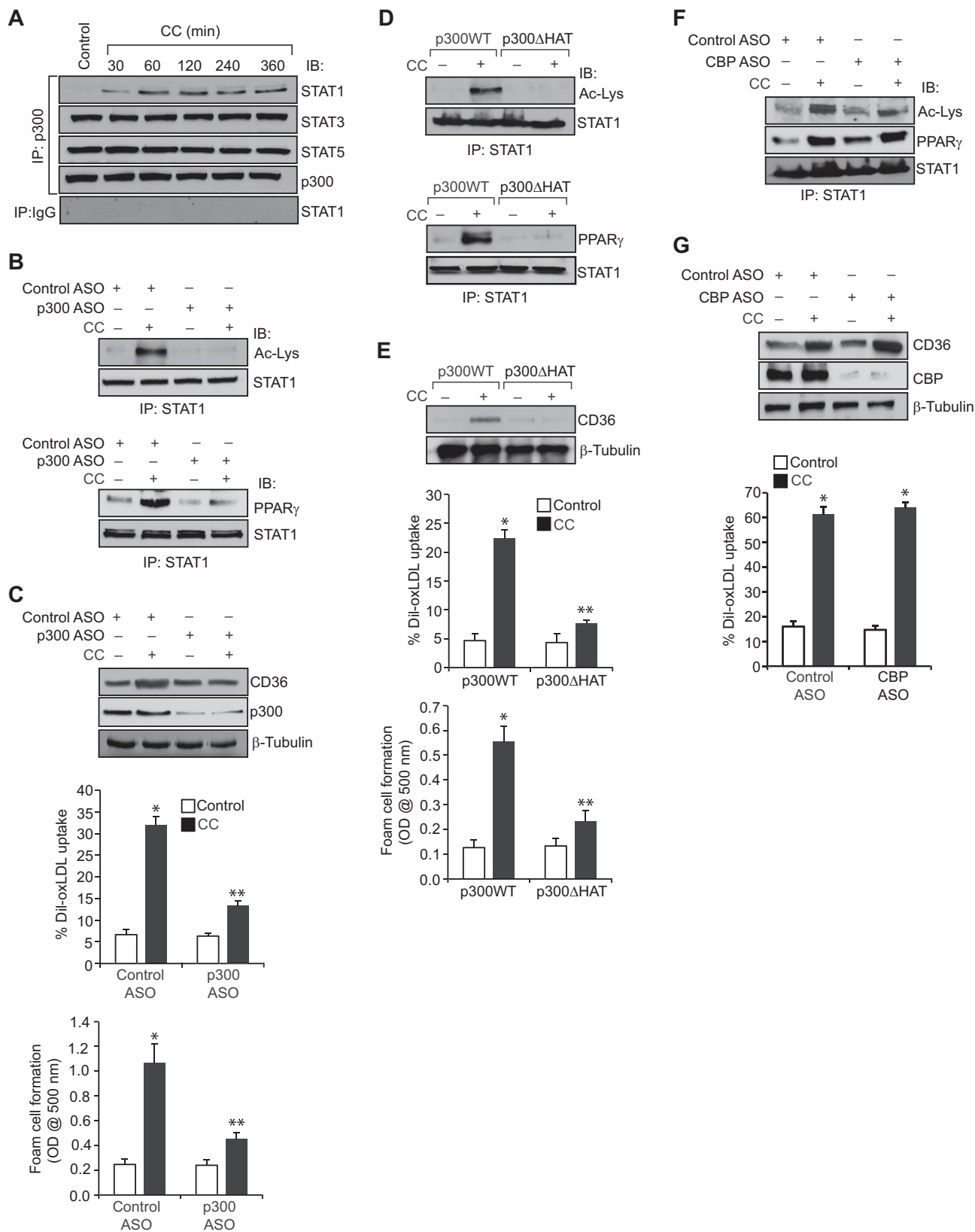
CC-induced p300 tyrosine phosphorylation, we first studied the time course effect of CC on tyrosine phosphorylation and activation of various NRTKs. CC while having little or no effect on Src and Syk tyrosine phosphorylation stimulated the tyrosine phosphorylation of BTK and Pyk2 in a time dependent manner (Fig. 4B). Based on these results we examined the role of BTK and Pyk2 in CC-induced p300 tyrosine phosphorylation, its association with STAT1, STAT1 acetylation and its interaction with PPAR γ in CD36 expression, oxLDL uptake and foam cell formation. Despite the robust activation of both BTK and Pyk2 by CC, downregulation of only BTK but not Pyk2 blunted CC-induced CD36 expression, oxLDL uptake and foam cell formation (Fig. 4C). In accordance with these observations, ASO-mediated depletion of BTK levels also blocked CC-induced p300 tyrosine phosphorylation, its association with STAT1, STAT1 acetylation and its interaction with PPAR γ (Fig. 4D). Furthermore, downregulation of BTK by its ASO inhibited p300 acetyltransferase activity (Fig. 4D).

3.5. Role of ROS in CC-induced BTK activation, p300 tyrosine phosphorylation, STAT1 acetylation and its interaction with PPAR γ in mediating CD36 expression, oxLDL uptake and foam cell formation

Previously, we have reported that ROS are involved in the activation of Syk and Pyk2 in 15(S)-HETE-induced p300 tyrosine phosphorylation, STAT1 acetylation and its interaction with PPAR γ in CD36 expression, oxLDL uptake and foam cell formation [27]. Therefore, we tested the role of ROS in CC-induced BTK activation, p300 tyrosine phosphorylation, STAT1 acetylation and its interaction with PPAR γ in CD36 expression, oxLDL uptake and foam cell formation. As measured by both CM-H2DCFDA and Amplex Red hydrogen peroxide/peroxidase assay kit methods, CC induced ROS production in a time dependent manner with a maximum fourfold increase at 30 min (Fig. 5A). NADPH and xanthine oxidases are the major sources of ROS production in many cell types [37,38]. Therefore, to find the source of CC-induced ROS production, we tested the role of NADPH oxidase and xanthine oxidase. We found that apocyanin and DPI, potent inhibitors of NADPH oxidase [37], and allopurinol, potent inhibitor of xanthine oxidase [37], substantially reduced CC-induced ROS production

(Fig. 5A). These observations infer that both NADPH oxidase and xanthine oxidase are involved in CC-induced ROS production. Consistent with these observations, ASO-mediated downregulation of p47Phox (a NADPH oxidase component) or xanthine oxidase levels suppressed CC-induced

CD36 expression, oxLDL uptake and foam cell formation (Fig. 5B). In line with the above findings, depletion of p47Phox or xanthine oxidase levels inhibited CC-induced BTK and p300 tyrosine phosphorylation, STAT1 acetylation and its interaction with PPAR γ (Fig. 5C). ASO-mediated



depletion of p47Phox or xanthine oxidase levels also inhibited p300 acetyltransferase activity (Fig. 5C).

3.6. STAT1, PPAR γ and p300 mediate CC-induced CD36 promoter activity

We have previously shown that STAT1, PPAR γ and p300 bind to a STAT-binding site in CD36 promoter and enhance its activity in response to a lipid hydroperoxide, 15(S)-HETE [27]. In lieu of these observations, we asked the question whether these transcriptional factors and coactivator have any role in CC-induced CD36 promoter activity. EMSA and supershift EMSA revealed that STAT1, PPAR γ and p300 bind to an oligonucleotide probe harboring the STAT-binding site at -107 nt in the CD36 promoter (Fig. 6A). In addition, ChIP and re-ChIP assays were conducted to determine the binding of STAT1, PPAR γ and p300 to the STAT-binding site at -107 nt in the CD36 promoter in intact cells. ChIP assay results showed that STAT1, PPAR γ and p300 bind to the same CD36 promoter region (Fig. 6B). Re-ChIP analysis of anti-STAT1 chromatin immunocomplexes further showed that PPAR γ and p300 bind to the CD36 promoter along with STAT1 (Fig. 6B). Conversely, re-ChIP analysis of anti-PPAR γ chromatin immunocomplexes revealed that STAT1 and p300 bind to CD36 promoter along with PPAR γ (Fig. 6B). Likewise, re-ChIP analysis of anti-p300 chromatin immunocomplexes showed that STAT1 and PPAR γ bind to the CD36 promoter along with p300 (Fig. 6B). In addition, while STAT1 tyrosine mutant PFS1YF had no effect, its acetyl mutant K410R/K413R blocked the recruitment of STAT1, PPAR γ and p300 to the CD36 promoter in response to CC (Fig. 6C). Similarly, p300 Δ HAT that lacks the acetyltransferase activity prevented CC-induced binding of STAT1, PPAR γ and p300 to the CD36 promoter (Fig. 6D). GW9662, the antagonist of PPAR γ , however while blocking CC-induced PPAR γ binding to the CD36 promoter had no effect on STAT1 or p300 binding (Fig. 6E). Depletion of BTK, p47Phox or xanthine oxidase levels also prevented CC-induced binding of STAT1, PPAR γ and p300 to the CD36 promoter (Fig. 6F and G). To confirm these results, we have transfected THP1 cells with pGL3 vector or pGL3 harboring ~800 bp CD36 promoter-luciferase reporter gene and studied their response to CC. CC induced CD36 promoter-luciferase reporter gene activity by 8-fold (Fig. 7A). In addition, site-directed mutagenesis of STAT-binding site at -107 nt blocked CC-induced CD36 promoter-luciferase reporter gene activity (Fig. 7A). Furthermore, CC-induced CD36 promoter-luciferase reporter gene activity was found to be sensitive to inhibition of NADPH oxidase, xanthine oxidase, BTK activation, STAT1 acetylation, PPAR γ activation and p300 HAT activity (Fig. 7B–F).

3.7. CC induces ROS production, BTK activation, p300-STAT1-PPAR γ interactions, CD36 expression and foam cell formation in mouse primary peritoneal macrophages

In order to validate the observations obtained in THP1 cells, we also studied the effects of CC on ROS production, BTK activation, p300 phosphorylation, STAT1 acetylation and its interactions with p300 and

PPAR γ , CD36 expression, oxLDL uptake and foam cell formation in mouse primary peritoneal macrophages. It is indeed exciting to find that CC induced ROS production, BTK and p300 tyrosine phosphorylation, p300 association with STAT1, STAT1 acetylation and its interaction with PPAR γ , CD36 expression, oxLDL uptake and foam cell formation in mouse primary peritoneal macrophages (Fig. 8A–E).

4. Discussion

Although scavenger receptor genes, particularly types A and B do not contain sterol regulatory elements, their expression is induced in response to high free and esterified intracellular cholesterol levels [39]. Because of this correlation between scavenger receptor expression and cellular cholesterol levels, these receptors are likely to play an important role in the uptake of oxLDL by macrophages during atherogenesis. Several studies have shown that in patients with high circulating levels of LDL-cholesterol, sub endothelial retention of LDL increases and creates a microenvironment in which it becomes oxidized, which is no longer recognized by the LDL-receptor, but rather becomes a ligand for scavenger receptors [40]. Therefore, scavenger receptor expression is likely a determinant factor for oxLDL uptake by cells such as macrophages. In this context, among the many scavenger receptors, CD36 has been shown to be a major mediator of oxLDL uptake and foam cell formation [25,27,41]. Despite the advancement in our understating between cellular cholesterol levels and scavenger receptor expression, the underlying mechanisms of their induction were not clear. In the present study, we report that CC stimulates CD36 expression leading to oxLDL uptake and foam cell formation. Previous work from others as well as our laboratory has shown that STAT1 plays a role in CD36 expression and foam cell formation [27,28]. Based on these observations, we hypothesized that STAT1 might be playing a role in CC-induced CD36 expression and foam cell formation. Indeed, our findings reveal that CC stimulates STAT1 tyrosine phosphorylation and acetylation in THP1 cells. However, despite the capacity of CC in the stimulation of both tyrosine phosphorylation and acetylation of STAT1 CC-induced CD36 expression, oxLDL uptake and foam cell formation showed a requirement only for STAT1 acetylation but not tyrosine phosphorylation. These observations are consistent with our previous findings on the role of STAT1 acetylation in lipid hydroperoxide 15(S)-HETE-induced CD36 expression, oxLDL uptake and foam cell formation.

Many studies have demonstrated that PPAR γ plays a role in CD36 expression and foam cell formation [33,34]. In addition, we have reported that 15(S)-HETE induces CD36 expression, oxLDL uptake and foam cell formation and these events require STAT1 acetylation and its interaction with PPAR γ [27]. In the present study, we also found that CC-induced CD36 expression, oxLDL uptake and foam cell formation require PPAR γ activation. Furthermore, our results show that acetylation-mediated STAT1 interaction with PPAR γ is needed for CC-induced CD36 expression, oxLDL uptake and foam cell formation. Since no interactions were observed between STAT3 or STAT5 with PPAR γ and CC had no influence on the interactions between STAT2, STAT4 or STAT6 with PPAR γ , it is unlikely that these STATs are

Fig. 3. CC-induced STAT1 acetylation requires p300 acetyltransferase activity. A. Equal amounts of protein from control and the indicated time periods of CC (40 μ g/ml)-treated cells were immunoprecipitated with anti-p300 antibodies or IgG and the immunocomplexes were analyzed by Western blotting for STAT1, STAT3, or STAT5 levels and normalized for p300. B. Quiescent cells were transfected with control or p300 ASO, quiesced, treated with and without CC for 1 h, cell extracts were prepared and equal amounts proteins from each condition were immunoprecipitated with anti-STAT1 antibodies and the immunocomplexes were analyzed by Western blotting for STAT1 acetylation and its association with PPAR γ as described in Fig. 1, panel F and Fig. 2, panel C, respectively. C. All the conditions were same as in panel B except that cells were treated with vehicle or CC and analyzed for CD36 expression, oxLDL uptake or foam cell formation as described in Fig. 1, panel C. The blot was re-probed for p300 and β -tubulin to show the effect of the ASO on its target and off target molecules levels. D and E. Cells were transfected with p300WT or p300 Δ HAT, quiesced, treated with and without CC and analyzed for STAT1 acetylation, its association with PPAR γ , CD36 expression, oxLDL uptake or foam cell formation as described above in panels B and C, respectively. The blots were re-probed for STAT1 or β -tubulin for normalization. F and G. Cells were transfected with control or CBP ASO, quiesced, treated with and without CC and analyzed for STAT1 acetylation and its association with PPAR γ , CD36 expression and oxLDL uptake as described above in panels B and C, respectively. The blots were re-probed for CBP, STAT1 or β -tubulin to show the effect of the ASO on its target and off target molecules levels. The bar graphs represent Mean \pm S.D. values of three experiments. * p < 0.01 vs control ASO or p300WT; ** p < 0.01 versus control ASO+CC or p300WT+CC.

involved in CC-induced CD36 expression, oxLDL uptake and foam cell formation. Similarly, because STAT1 tyrosine phosphorylation was not required for CC-induced CD36 expression, a slight increase in STAT2, STAT3 or STAT6 tyrosine phosphorylation by CC may also be not linked to this scavenger receptor expression by CC. Many studies have shown that p300 mediates acetylation of STATs, particularly STAT1 and STAT3 [30–32]. While exploring the mechanisms of STAT1 acetylation by CC, we observed that CC stimulates tyrosine phosphorylation and activation of p300, which in turn, mediates STAT1 acetylation and its interaction with PPAR γ . Several reports showed that p300 activation depends on its Ser/Thr phosphorylation [42]. However, our findings reveal that CC stimulates p300 tyrosine phosphorylation rather than Ser/Thr phosphorylation leading to its activation. Previously, we have reported that Syk and Pyk2 mediate 15(S)-HETE-induced tyrosine phosphorylation of p300 leading to its activation and its role in STAT1 acetylation and its interaction with PPAR γ in CD36 expression, oxLDL uptake and foam cell formation. In contrast to

these observations, the present findings show that CC while having little or no effect on Src and Syk activation stimulate BTK and Pyk2 tyrosine phosphorylation. Interestingly, while Pyk2 depletion had no effect, down regulation of BTK levels attenuated CC-induced p300 tyrosine phosphorylation, STAT1 acetylation and its interaction with PPAR γ resulting in reduced CD36 expression, oxLDL uptake and foam cell formation. BTK is a member of the Tec family of non-receptor tyrosine kinases and plays an important role in B-lymphocyte differentiation and signaling [43]. It has also been demonstrated that BTK-deficient mice display a reduced leukocyte recruitment and inflammatory response in various disease models [44]. Furthermore, the absence of functional BTK increases the tendency of macrophages to undergo apoptosis and as a result diminishes their proinflammatory functions [45]. Despite the large number of studies on the role of BTK in cancer and inflammatory diseases [46,47], very little is known on its role in vascular diseases. Toward this end, the present findings reveal that BTK via tyrosine phosphorylation and activation of p300 and thereby

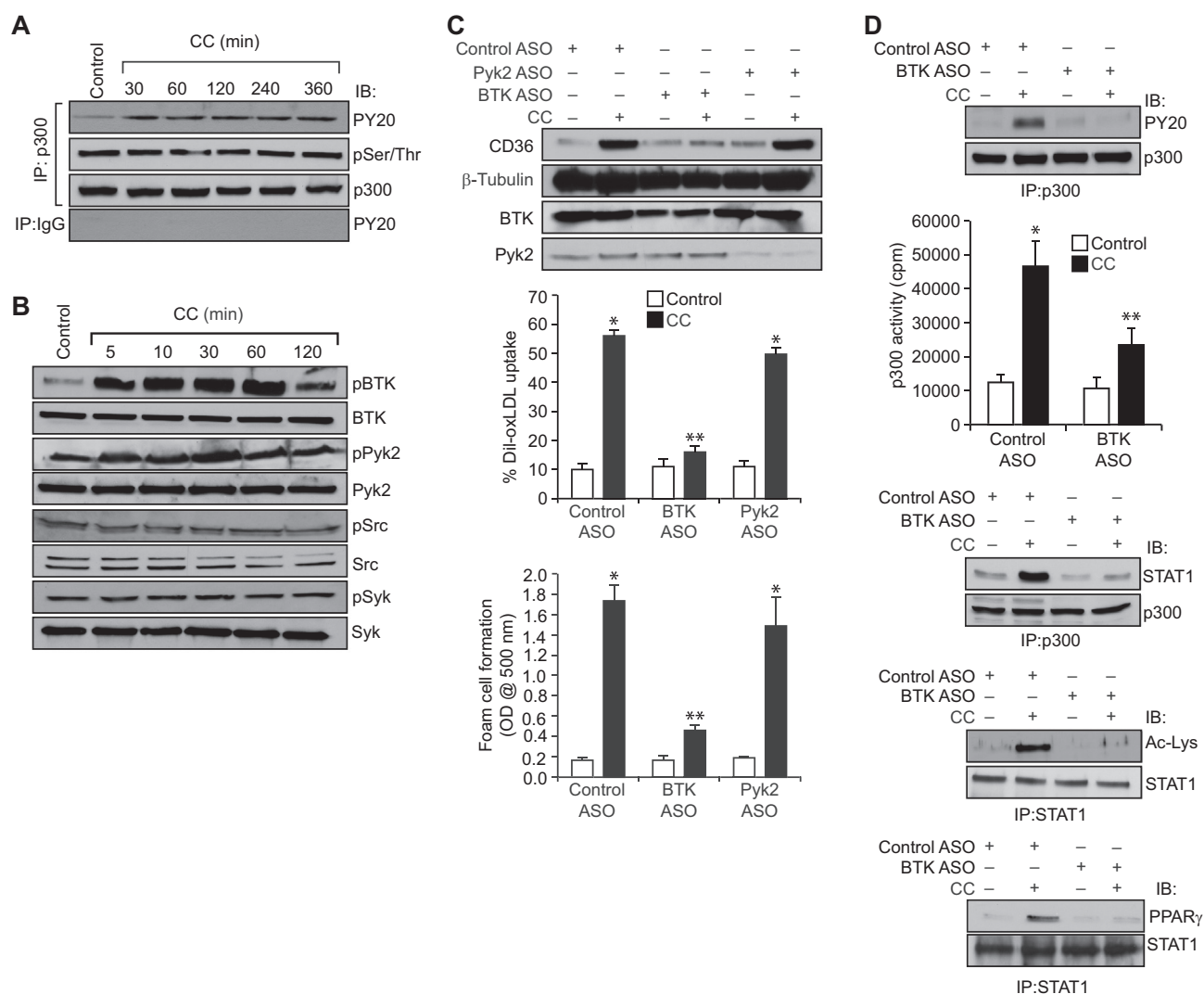


Fig. 4. CC induces p300 activation in BTK-dependent manner. **A.** Equal amounts of protein from control and the indicated time periods of CC (40 μ g/ml)-treated cells were immunoprecipitated with anti-p300 antibodies or IgG and the immunocomplexes were analyzed by Western blotting with anti-PY20 or anti-phosphoserine/threonine antibodies followed by normalization for p300. **B.** All the conditions were same as in panel A except that the cell extracts were analyzed by Western blotting for pBTK, pPyk2, pSrc and pSyk levels using their phospho-specific antibodies and normalized for their total levels. **C.** Cells were transfected with the indicated ASO, quiesced, treated with and without CC and analyzed for CD36 expression, oxLDL uptake or foam cell formation as described in Fig. 1, panel C. The blot was reprobed for BTK, Pyk2 and β -tubulin levels to show the effects of the ASOs on their target and off target molecules levels. **D.** Cells were transfected with control or BTK ASO, quiesced, treated with and without CC for 1 h and cell extracts were prepared. Equal amount of protein from control and each treatment were immunoprecipitated with anti-p300 or anti-STAT1 antibodies and the immunocomplexes were analyzed by Western blotting for anti-PY20, anti-STAT1, anti-Ac-Lys or anti-PPAR γ antibodies and normalized for p300 or STAT1. An equal amount of protein from control and each treatment was also assayed for p300 acetyltransferase activity. * $p < 0.01$ vs control ASO; ** $p < 0.01$ vs control ASO+CC.

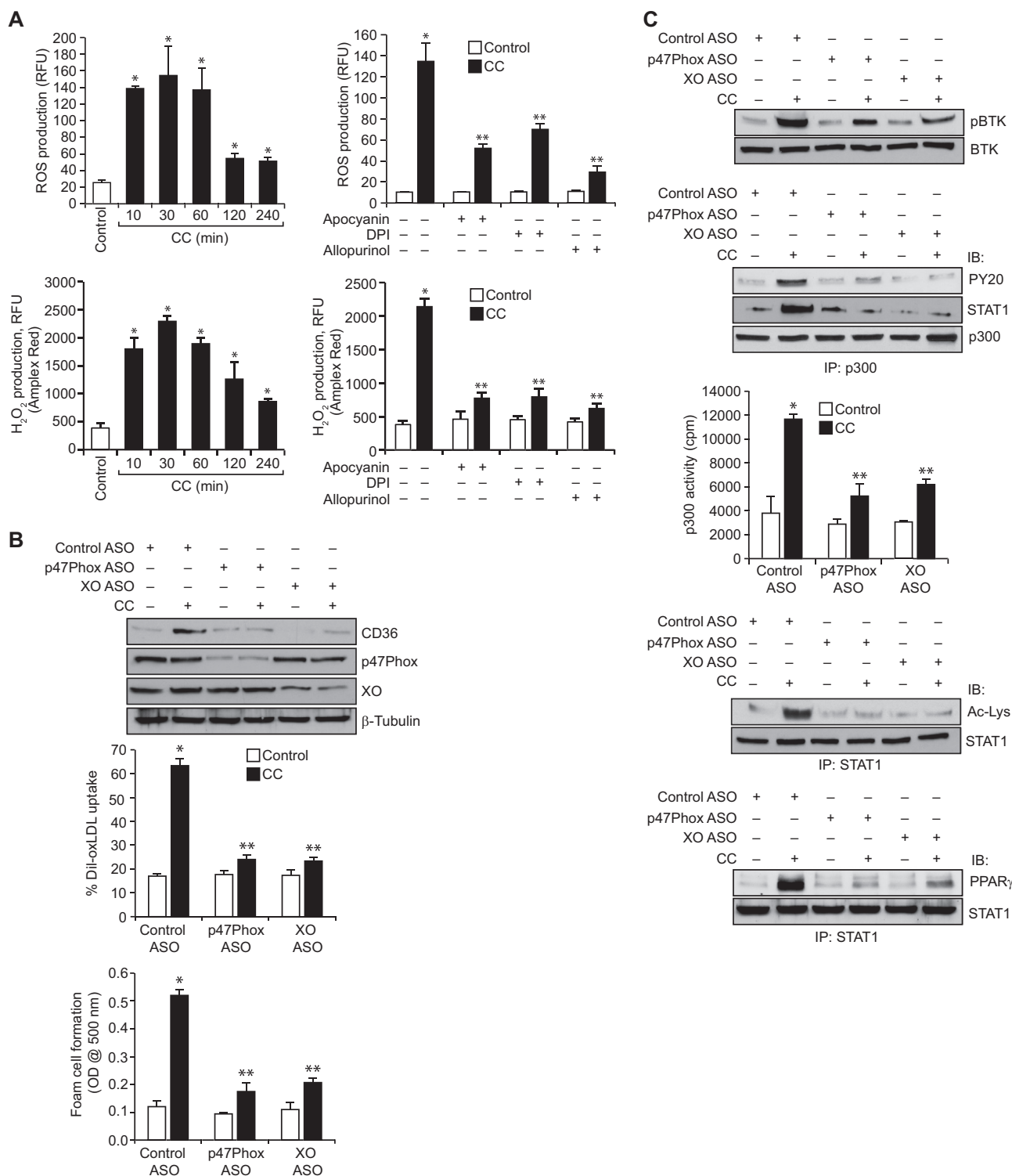


Fig. 5. CC-induced BTK activation depends on NADPH and xanthine oxidases-mediated ROS production. A. Quiescent cells were treated with vehicle or CC (40 μg/ml) for the indicated time periods or for 30 min in the presence and absence of Apocyanin (100 μM), DPI (10 μM) or Allopurinol (100 μM) and ROS production was measured using CM-H2DCFDA and Amplex Red. B. Cells were transfected with control, p47Phox or xanthine oxidase ASOs, quiesced, treated with vehicle or CC and analyzed for CD36 expression, oxLDL uptake or foam cell formation as described in Fig. 1, panel C. The CD36 blot was reprobed for p47Phox, xanthine oxidase and β-tubulin levels to show the effects of the ASOs on their target and off target molecules levels or normalization. C. Cells that were transfected with control, p47Phox or xanthine oxidase ASOs and quiesced were treated with vehicle or CC for 1 h and analyzed for BTK and p300 tyrosine phosphorylation, p300 association with STAT1, STAT1 acetylation and its interaction with PPAR_γ as described in Fig. 4, panels B, A and D, respectively, and the blots were reprobed for BTK, p300 or STAT1 levels for normalization. An equal amount of protein from control and each treatment was also assayed for p300 acetyltransferase activity. *p < 0.01 vs control ASO; **p < 0.01 vs CC or control ASO+CC.

facilitating STAT1 acetylation and its interaction with PPAR_γ plays an important role in CC-induced CD36 expression, oxLDL uptake and foam cell formation. Based on these observations a role for BTK in the

pathogenesis of atherosclerosis may also be suggested. In this context, it is worth pointing that a recent study has shown that BTK mediates NLRP3-dependent inflammasome formation [47]. Since CC also trigger

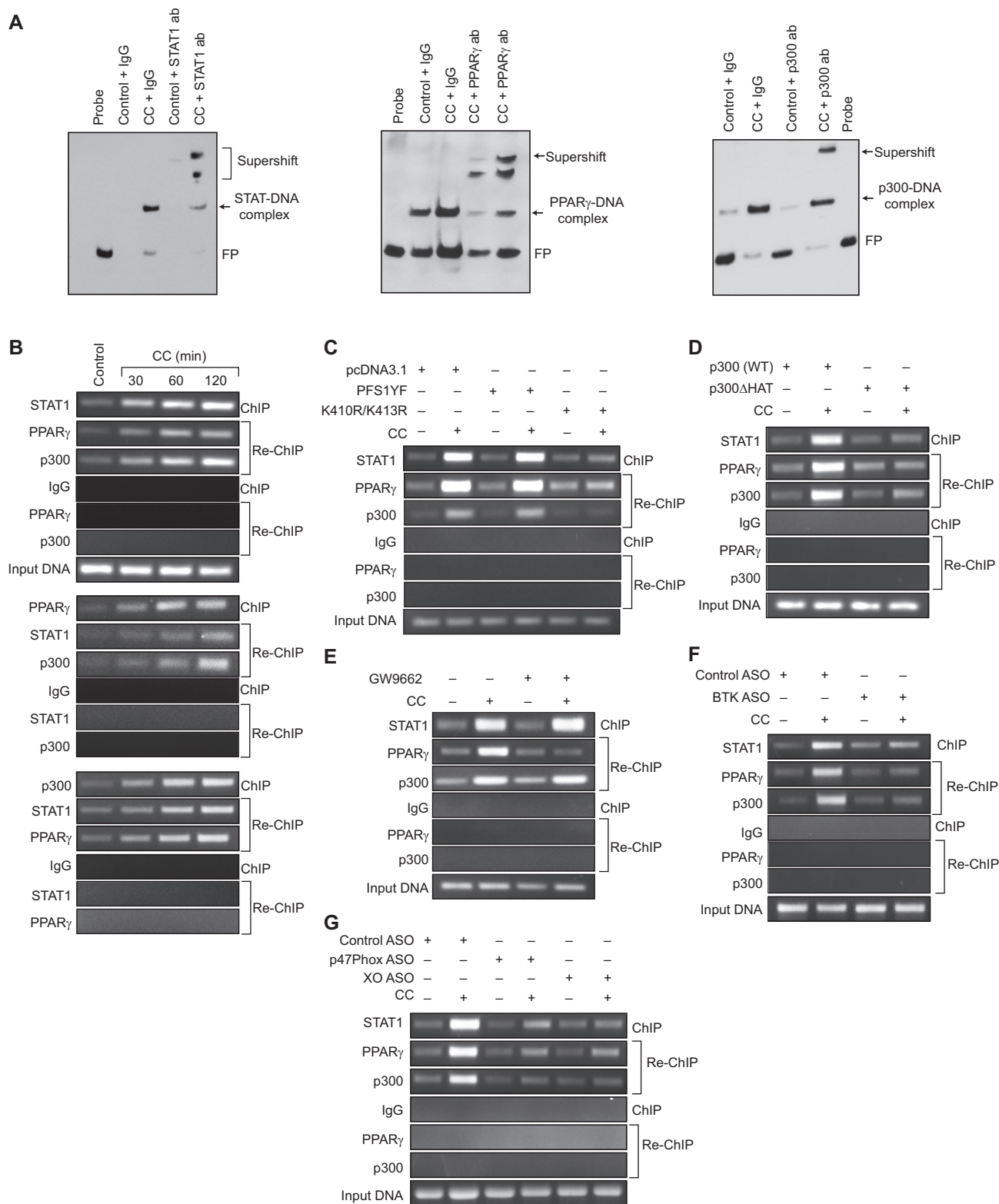


Fig. 6. Interactions between STAT1, PPAR γ and p300 are required for CC-induced STAT1 binding to CD36 promoter. **A.** Nuclear extracts of control and 2 h of CC (40 μ g/ml)-treated cells were analyzed by EMSA and supershift EMSA for the presence of STAT1, PPAR γ and p300 in the STAT-DNA complexes using STAT binding site at -107 nt in the CD36 promoter as a biotin-labeled probe. **B.** Quiescent cells were treated with vehicle or CC for the indicated time periods and subjected to ChIP and re-ChIP assays of CD36 promoter using anti-STAT1, anti-PPAR γ or anti-p300 antibodies with the indicated sequential order. **C** and **D.** Cells were transfected with vector, PFS1YF, K410R/K413R, p300WT or p300 Δ HAT, quiesced, treated with and without CC for 2 h and subjected to ChIP and re-ChIP assays for STAT1, PPAR γ and p300 binding to CD36 promoter as described in panel B. **E.** Quiescent cells were treated with vehicle or CC in the presence and absence of GW9662 (5 μ M) for 2 h and subjected to ChIP and re-ChIP assays for STAT1, PPAR γ and p300 binding to CD36 promoter as described in panel B. **F** and **G.** Cells were transfected with the indicated ASOs, quiesced, treated with and without CC for 2 h and subjected to ChIP and re-ChIP assays for STAT1, PPAR γ and p300 binding to CD36 promoter as described in panel B. IgG was used as a negative control.

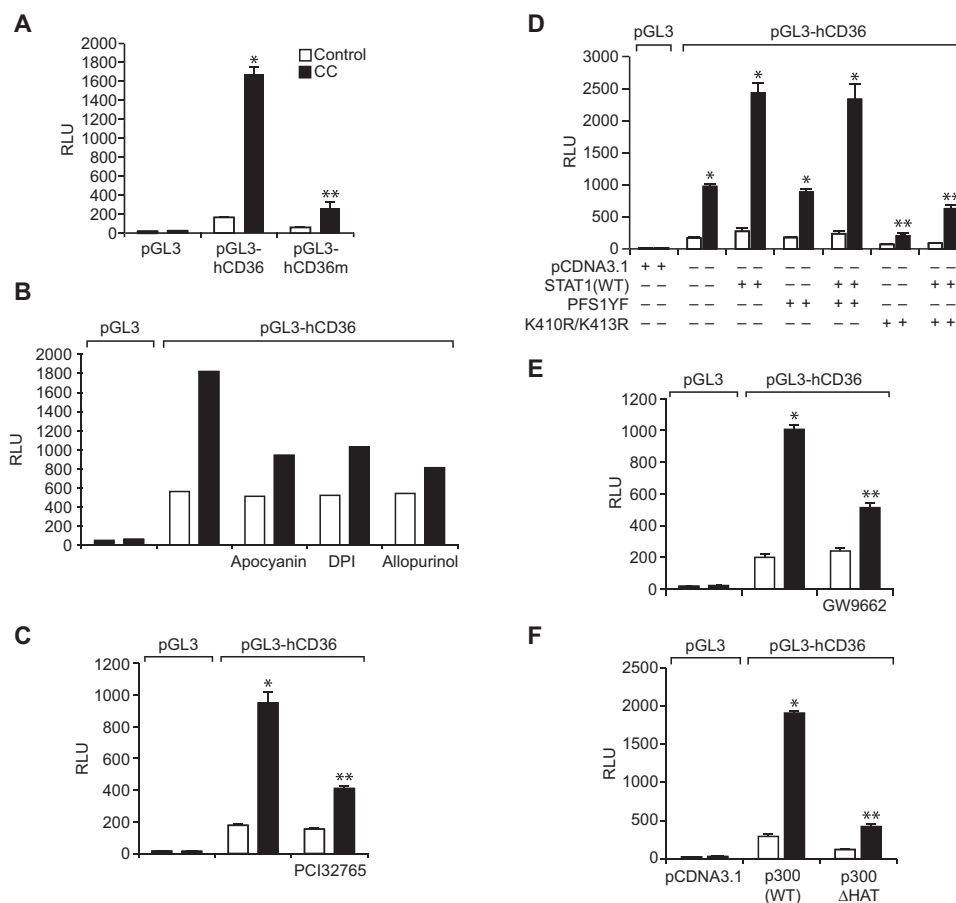


Fig. 7. STAT1, PPAR γ and p300 mediate CC-induced CD36 promoter activity. A. Cells were transfected with vector, pGL3-hCD36 or pGL3-hCD36m (STAT-binding site at -107 nt was mutated), growth-arrested, treated with and without CC (40 μ M) for 6 h and the luciferase activity was measured. B, C and E. After transfection with vector or pGL3-hCD36, cells were quiesced, treated with vehicle or CC in the presence and absence of Apocyanin (100 μ M), DPI (10 μ M), Allopurinol (100 μ M), PCI32765 (10 μ M) or GW9662 (5 μ M) for 6 h and the luciferase activity was measured. D and F. Cells were co-transfected with vector or pGL3-hCD36 in combination with pcDNA3.1, PFS1YF, K410R/K413R, p300WT or p300 Δ HAT, quiesced, treated with vehicle or CC for 6 h and the luciferase activity was measured. * $p < 0.01$ vs vector; ** $p < 0.01$ vs vector+CC or STAT1+CC or p300WT+CC. RLU, relative luciferase units.

NLRP3-mediated inflammasome formation [12], it is quite possible that BTK besides its role in CC-induced CD36 expression and foam cell formation may also be involved in CC-induced inflammasome formation in the pathogenesis of atherosclerosis.

A large body of data suggests that oxidative stress plays a notable role in atherogenesis [48,49]. It has been demonstrated that macrophages from hypercholesterolemic patients show enhanced ROS production and proinflammatory cytokine expression as compared to control macrophages [50,51]. In this aspect, the present findings demonstrate that CC induces ROS production leading to activation of BTK. These observations also infer that CC via ROS production and activation of BTK stimulates a transcriptional machinery involving p300-STAT1-PPAR γ in inducing proatherogenic genes such as CD36 expression. The EMSA, supershift EMSA, ChIP, re-ChIP and promoter-reporter gene analysis further support these conclusions. The re-ChIP analysis of anti-PPAR γ chromatin immunoprecipitates revealed that activation of PPAR γ is not required for the binding of STAT1 or p300 to the CD36 promoter. These results suggest that p300-mediated STAT1 acetylation rather than PPAR γ activation is crucial for the binding of STAT1-PPAR γ complexes to the CD36 promoter. Because PPAR γ antagonist inhibits the PPAR γ binding to the CD36 promoter and attenuates the promoter activity partially, it is quite possible that in addition to its involvement in STAT1-mediated promoter activity, PPAR γ alone might be involved in the regulation of CD36 promoter activity and its expression at least partially. It is worth to note that both

XO and NADPH oxidase were involved in CC-induced ROS production in the modulation of CD36 expression and foam cell formation. Previously, we have reported that an interaction between XO and NADPH oxidase is required for 15(S)-HETE-induced ROS production and IL17A expression in mediating monocyte migration and its adhesion to endothelial cells [21]. Based on these observations, it may be suggested that an interdependent activation of XO and NADPH oxidase is involved in CC-induced ROS production leading to CD36 expression and foam cell formation. Although the present results do not address the role of mitochondrial ROS in CC-induced CD36 expression and foam cell formation, it is possible that XO and NADPH oxidase-mediated ROS production could trigger mitochondrial ROS production in this scavenger receptor expression and foam cell formation by CC, which remains to be explored.

As ubiquitous component of cell membranes, cholesterol plays an important role in the maintenance of membrane structure and function, particularly membrane fluidity and cell signaling [52]. Previous studies have suggested that endogenous molecules trigger inflammation driving the atherosclerotic lesion development and one of those suspects is cholesterol [14–16]. Cholesterol is known to accumulate in atherosclerotic plaques in the form of cholesterol crystals in foam cells [14,15]. In addition to this information, the present results as summarized in Fig. 9 reveal that CC via XO and NADPH oxidase-dependent ROS production and BTK activation leads to p300 tyrosine phosphorylation and activation, which in turn, by acetylating STAT1

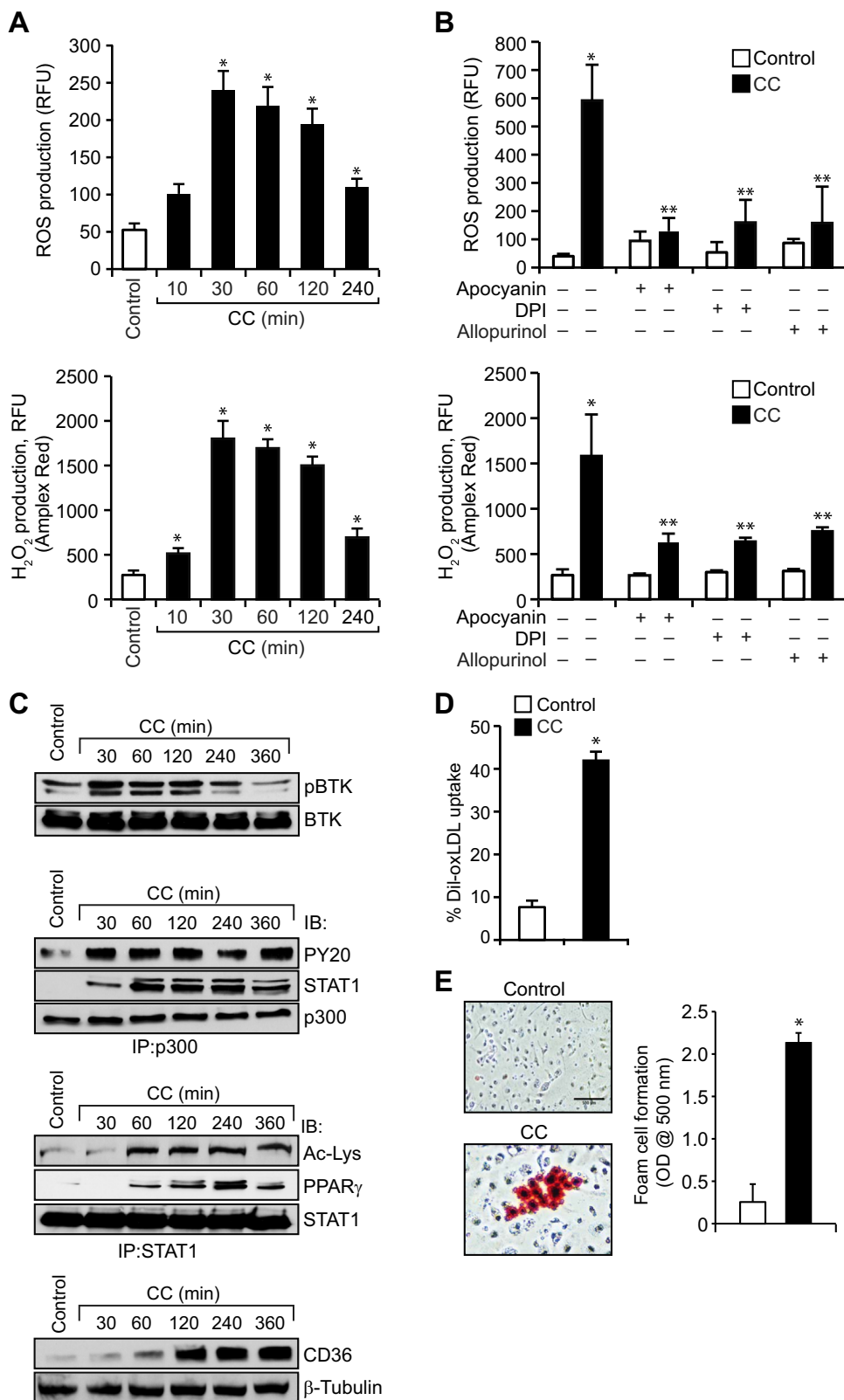


Fig. 8. CC induces ROS production, BTK activation, p300-STAT1-PPAR γ interactions, CD36 expression and foam cell formation in mouse primary peritoneal macrophages. A–C. Mouse primary peritoneal macrophages were isolated from WT mice, quiesced overnight, treated with and without CC (40 μ g/ml) for the indicated time periods and either ROS production was measured or cell extracts were prepared and analyzed for BTK and p300 tyrosine phosphorylation, p300 association with STAT1, STAT1 acetylation and its association with PPAR γ and CD36 expression as described in Figure legends 5A, 4B, 4A, 3A, 1F, 2B and 1A, respectively. D and E. Mouse primary peritoneal macrophages after overnight growth arrest were treated with and without CC (40 μ g/ml) for 6 h and analyzed for oxLDL uptake and foam cell formation as described in Figure legend 1 C. *p < 0.01 vs control.

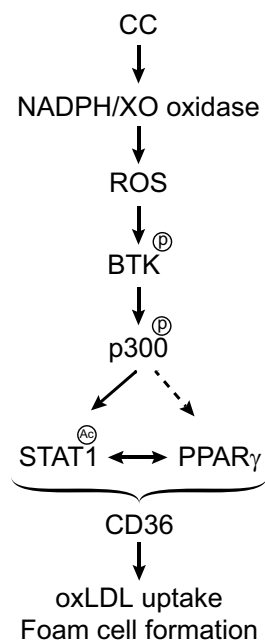


Fig. 9. Schematic diagram shows the potential mechanisms of CD36 expression and foam cell formation by cholesterol crystals.

facilitates STAT1 interaction with PPAR γ in mediating CD36 expression, oxLDL uptake and foam cell formation.

Conflict of interest

The authors have no conflict of interest to declare.

Acknowledgements

This work was supported by HL064165 grant from NHLBI to GNR.

References

- G.K. Hansson, A. Hermansson, The immune system in atherosclerosis, *Nat. Immunol.* 12 (2011) 204–212.
- P. Libby, P.M. Ridker, G.K. Hansson, Progress and challenges in translating the biology of atherosclerosis, *Nature* 473 (2011) 317–325.
- L. Demer, Y. Tintut, The roles of lipid oxidation products and receptor activator of nuclearfactor- κ B signaling in atherosclerotic calcification, *Circ. Res.* 108 (2011) 1482–1493.
- D. Steinberg, Lipoproteins and the pathogenesis of atherosclerosis, *Circulation* 76 (1987) 508–514.
- A. Pearson, A. Lux, M. Krieger, Expression cloning of dSR-C1, a class C macrophage-specific scavenger receptor from *Drosophila melanogaster*, *Proc. Natl. Acad. Sci. USA* 92 (1995) 4056–4060.
- A. Rigotti, S.L. Acton, M. Krieger, The class B scavenger receptors SR-BI and CD36 are receptors for anionic phospholipids, *J. Biol. Chem.* 270 (1995) 16221–16224.
- G. Endemann, L.W. Stanton, K.S. Madden, C.M. Bryant, R.T. White, A.A. Protter, CD36 is a receptor for oxidized low density lipoprotein, *J. Biol. Chem.* 268 (1993) 11811–11816.
- A.C. Nicholson, S. Frieda, A. Pearce, R.L. Silverstein, Oxidized LDL binds to CD36 on human monocyte-derived macrophages and transfected cell lines. Evidence implicating the lipid moiety of the lipoprotein as the binding site, *Arterioscler. Thromb. Vasc. Biol.* 15 (1995) 269–275.
- S. Cho, CD36 as a therapeutic target for endothelial dysfunction in stroke, *Curr. Pharm. Des.* 18 (2012) 3721–3730.
- N.N. Tandon, U. Kralisz, G.A. Jamieson, Identification of glycoprotein IV (CD36) as a primary receptor for platelet-collagen adhesion, *J. Biol. Chem.* 264 (1989) 7576–7583.
- V. Christiaens, M. Van Hul, H.R. Lijnen, I. Scroyen, CD36 promotes adipocyte differentiation and adipogenesis, *Biochim. Biophys. Acta* 1820 (2012) 949–956.
- P. Duewell, H. Kono, K.J. Rayner, C.M. Sirois, G. Vladimer, F.G. Bauernfeind, G.S. Abela, L. Franchi, G. Nuñez, M. Schnurr, T. Espevik, E. Lien, K.A. Fitzgerald, K.L. Rock, K.J. Moore, S.D. Wright, V. Hornung, E. Latz, NLRP3 inflammasomes are required for atherogenesis and activated by cholesterol crystals, *Nature* 464 (2010) 1357–1361.
- R. Virmani, F.D. Kolodgie, A.P. Burke, A. Farb, S.M. Schwartz, Lessons from

- sudden coronary death: a comprehensive morphological classification scheme for atherosclerotic lesions, *Arterioscler. Thromb. Vasc. Biol.* 20 (2000) 1262–1275.
- G.S. Abela, Cholesterol crystals piercing the arterial plaque and intima trigger local and systemic inflammation, *J. Clin. Lipidol.* 4 (2010) 156–164.
- F.D. Kolodgie, A.P. Burke, G. Nakazawa, Q. Cheng, X. Xu, R. Virmani, Free cholesterol in atherosclerotic plaques: where does it come from?, *Curr. Opin. Lipidol.* 18 (2007) 500–507.
- E.O. Samstad, N. Niyonzima, S. Nymo, M.H. Aune, L. Ryan, S.S. Bakke, K.T. Lappegård, O.L. Brekke, J.D. Lambris, J.K. Damás, E. Latz, T.E. Mollnes, T. Espevik, Cholesterol crystals induce complement-dependent inflammasome activation and cytokine release, *J. Immunol.* 192 (2014) 2837–2845.
- C.J. Binder, N. Papac-Milicevic, J.L. Witztum, Innate sensing of oxidation-specific epitopes in health and disease, *Nat. Rev. Immunol.* 16 (2016) 485–497.
- J. Han, D.P. Hajjar, J.M. Tauras, A.C. Nicholson, Cellular cholesterol regulates expression of the macrophage type B scavenger receptor, CD36, *J. Lipid Res.* 40 (1999) 830–838.
- J. Feng, J. Han, S.F. Pearce, R.L. Silverstein, A.M. Gotto Jr, D.P. Hajjar, A.C. Nicholson, Induction of CD36 expression by oxidized LDL and IL-4 by a common signaling pathway dependent on protein kinase C and PPAR- γ , *J. Lipid Res.* 41 (2000) 688–696.
- G.L. Flynn, Y. Shah, S. Prakongpan, K.H. Kwan, W.I. Higuchi, A.F. Hofmann, Cholesterol solubility in organic solvents, *J. Pharm. Sci.* 68 (1979) 1090–1097.
- S. Kotla, N.K. Singh, M.R. Heckle, G.J. Tigyi, G.N. Rao, The transcription factor CREB enhances interleukin-17A production and inflammation in a mouse model of atherosclerosis, *Sci. Signal.* 6 (2013) (ra83).
- M. Zhou, Z. Diwu, N. Panchuk-Voloshina, R.P. Haugland, A stable nonfluorescent derivative of resorufin for the fluorometric determination of trace hydrogen peroxide: applications in detecting the activity of phagocyte NADPH oxidase and other oxidases, *Anal. Biochem.* 253 (1997) 162–168.
- S. Kotla, N.K. Singh, J.G. Traylor Jr, A.W. Orr, G.N. Rao, ROS-dependent Syk and Pyk2-mediated STAT1 activation is required for 15(S)-hydroxyecosatetraenoic acid-induced CD36 expression and foam cell formation, *Free Radic. Biol. Med.* 76 (2014) 147–162.
- J.E. McLaren, D.R. Michael, R.C. Salter, T.G. Ashlin, C.J. Calder, A.M. Miller, F.Y. Liew, D.P. Ramji, IL-33 reduces macrophage foam cell formation, *J. Immunol.* 185 (2010) 1222–1229.
- S.O. Rahaman, W. Swat, M. Febbraio, R.L. Silverstein, Vav family Rho guanine nucleotide exchange factors regulate CD36-mediated macrophage foam cell formation, *J. Biol. Chem.* 286 (2011) 7010–7017.
- M. Febbraio, E.A. Podrez, J.D. Smith, D.P. Hajjar, S.L. Hazen, H.F. Hoff, K. Sharma, R.L. Silverstein, Targeted disruption of the class B scavenger receptor CD36 protects against atherosclerotic lesion development in mice, *J. Clin. Invest.* 105 (2000) 1049–1056.
- S. Kotla, G.N. Rao, Reactive oxygen species (ROS) Mediate p300-dependent STAT1 protein interaction with peroxisome proliferator-activated receptor (PPAR)- γ in CD36 protein expression and foam cell formation, *J. Biol. Chem.* 290 (2015) 30306–30320.
- S. Agrawal, M. Febbraio, E. Podrez, M.K. Cathcart, G.R. Stark, G.M. Chisolm, Signal transducer and activator of transcription 1 is required for optimal foam cell formation and atherosclerotic lesion development, *Circulation* 115 (2007) 2939–2947.
- Y.Y. Wu, R.A. Bradshaw, Activation of the Stat3 signaling pathway is required for differentiation by interleukin-6 in PC12-E2 cells, *J. Biol. Chem.* 275 (2000) 2147–2156.
- Z.L. Yuan, Y.J. Guan, D. Chatterjee, Y.E. Chin, Stat3 dimerization regulated by reversible acetylation of a single lysine residue, *Science* 307 (2005) 269–273.
- O.H. Krämer, S.K. Knauer, G. Greiner, E. Jandt, S. Reichardt, K.H. Gührs, R.H. Stauber, F.D. Böhmer, T. Heinzel, A phosphorylation-acetylation switch regulates STAT1 signaling, *Genes Dev.* 23 (2009) 223–235.
- V. Kundumani-Sridharan, D. Van Quyen, J. Subramani, N.K. Singh, Y.E. Chin, G.N. Rao, Novel interactions between NFATc1 (Nuclear Factor of Activated T cells c1) and STAT-3 (Signal Transducer and Activator of Transcription-3) mediate G protein-coupled receptor agonist, thrombin-induced biphasic expression of cyclin D1, with first phase influencing cell migration and second phase directing cell proliferation, *J. Biol. Chem.* 287 (2012) 22463–22482.
- L. Nagy, P. Tontonoz, J.G. Alvarez, H. Chen, R.M. Evans, Oxidized LDL regulates macrophage gene expression through ligand activation of PPAR γ , *Cell* 93 (1998) 229–240.
- J.T. Huang, J.S. Welch, M. Ricote, C.J. Binder, T.M. Willson, C. Kelly, J.L. Witztum, C.D. Funk, D. Conrad, C.K. Glass, Interleukin-4-dependent production of PPAR- γ ligands in macrophages by 12/15-lipoxygenase, *Nature* 400 (1999) 378–382.
- A. Szanto, L. Nagy, Retinoids potentiate peroxisome proliferator-activated receptor gamma action in differentiation, gene expression, and lipid metabolic processes in developing myeloid cells, *Mol. Pharmacol.* 67 (2005) 1935–1943.
- L.F. Chen, Y. Mu, W.C. Greene, Acetylation of RelA at discrete sites regulates distinct nuclear functions of NF κ B, *EMBO J.* 21 (2002) 6539–6548.
- R.A. Oeckler, P.M. Kaminski, M.S. Wolin, Stretch enhances contraction of bovine coronary arteries via an NAD(P)H oxidase-mediated activation of the extracellular signal-regulated kinase mitogen-activated protein kinase cascade, *Circ. Res.* 92 (2003) 23–31.
- A. Bhattacharyya, R. Chattopadhyay, S. Mitra, S.E. Crowe, Oxidative stress: an essential factor in the pathogenesis of gastrointestinal mucosal diseases, *Physiol. Rev.* 94 (2014) 329–354.
- P. Dawson, S. Hofmann, D. van de Westhuyzen, T. Sudhof, M. Brown, J. Goldstein, Sterol-dependent repression of low density lipoprotein receptor promoter mediated

- by 16-base pair sequence adjacent to binding site for transcription factor Sp1, *J. Biol. Chem.* 263 (1988) 3372–3379.
- [40] K.J. Williams, I. Tabas, The response-to-retention hypothesis of early atherogenesis, *Arterioscler. Thromb. Vasc. Biol.* 15 (1995) 551–561.
- [41] E.A. Podrez, M. Febbraio, N. Sheibani, D. Schmitt, R.L. Silverstein, D.P. Hajjar, P.A. Cohen, W.A. Frazier, H.F. Hoff, S.L. Hazen, Macrophage scavenger receptor CD36 is the major receptor for LDL modified by monocyte-generated reactive nitrogen species, *J. Clin. Invest.* 105 (2000) 1095–1108.
- [42] Y. Liu, C.E. Denlinger, B.K. Rundall, P.W. Smith, D.R. Jones, Suberoylanilide hydroxamic acid induces Akt-mediated phosphorylation of p300, which promotes acetylation and transcriptional activation of RelA/p65, *J. Biol. Chem.* 281 (2006) 31359–31368.
- [43] A.J. Mohamed, L. Yu, C.M. Bäckesjö, L. Vargas, R. Faryal, A. Aints, B. Christensson, A. Berglöf, M. Vihinen, B.F. Nore, C.I. Smith, Bruton's tyrosine kinase (Btk): function, regulation, and transformation with special emphasis on the PH domain, *Immunol. Rev.* 228 (2009) 58–73.
- [44] A. Mangla, A. Khare, V. Vineeth, N.N. Panday, A. Mukhopadhyay, B. Ravindran, V. Bal, A. George, S. Rath, Pleiotropic consequences of Bruton tyrosine kinase deficiency in myeloid lineages lead to poor inflammatory responses, *Blood* 104 (2004) 1191–1197.
- [45] F.M. Uckun, Bruton's tyrosine kinase (BTK) as a dual-function regulator of apoptosis, *Biochem. Pharmacol.* 56 (1998) 683–691.
- [46] L. Vargas, A. Hamasy, B.F. Nore, C.I. Smith, Inhibitors of BTK and ITK: state of the new drugs for cancer, autoimmunity and inflammatory diseases, *Scand. J. Immunol.* 78 (2013) 130–139.
- [47] M. Ito, T. Shichita, M. Okada, R. Komine, Y. Noguchi, A. Yoshimura, R. Morita, Bruton's tyrosine kinase is essential for NLRP3 inflammasome activation and contributes to ischaemic brain injury, *Nat. Commun.* 6 (2015) 7360.
- [48] H. Liu, R. Colavitti, I.I. Rovira, T. Finkel, Redox-dependent transcriptional regulation, *Circ. Res.* 97 (2005) 967–974.
- [49] D.I. Brown, K.K. Griendling, Regulation of signal transduction by reactive oxygen species in the cardiovascular system, *Circ. Res.* 116 (2015) 531–549.
- [50] H. Cai, D.G. Harrison, Endothelial dysfunction in cardiovascular diseases: the role of oxidant stress, *Circ. Res.* 87 (2000) 840–844.
- [51] A. Rezaie-Majd, T. Maca, R.A. Bucek, P. Valent, M.R. Müller, P. Husslein, A. Kashaipour, E. Minar, M. Baghestanian, Simvastatin reduces expression of cytokines interleukin-6, interleukin-8, and monocyte chemoattractant protein-1 in circulating monocytes from hypercholesterolemic patients, *Arterioscler. Thromb. Vasc. Biol.* 22 (2002) 1194–1199.
- [52] M.G. Sorci-Thomas, M.J. Thomas, Microdomains, inflammation, and atherosclerosis, *Circ. Res.* 118 (2016) 679–691.